RSC Advances

PAPER

View Article Online
View Journal | View Issue

Cite this: *RSC Adv.*, 2017, **7**, 38279

Preparation of cationic polymeric nanoparticles as an effective adsorbent for removing diclofenac sodium from water

Tao Liu, Zhihai Xie,* Yu Zhang, Jin Fan and Qing Liu

New cationic polymeric nanoparticles (PNPs) were synthesized by precipitation polymerization using [2-(methacryloyloxy)ethyl] trimethylammonium chloride and ethylene glycol dimethacrylate for adsorption of diclofenac sodium. The PNPs were characterized using FTIR, SEM, TEM, and their specific surface areas and thermal stabilities were measured. The adsorption capacity of PNPs was studied by static adsorption experiments. The adsorption equilibrium was achieved within only 7 min, and quantitative desorption required 3 min using 0.1 mol L^{-1} NaOH/methanol (1 : 1, v/v) as eluent. The maximum adsorption capacity of the PNPs for diclofenac sodium was 334.2 mg g^{-1}. The specific surface area for the PNPs was 192.5 m^2 g^{-1}. The isothermal adsorption model and the kinetic model were well fitted with the Langmuir adsorption model and a pseudo-second order kinetic model, and the adsorption mechanism was also discussed in detail. The PNPs could be used repeatedly for 6 cycles without a significant decrease in adsorption capacity. The prepared PNPs can be considered to be a promising sorbent for the adsorption of diclofenac sodium from water samples.

Received 16th June 2017
Accepted 28th July 2017

DOI: 10.1039/c7ra06730e

rsc.li/rsc-advances

1 Introduction

Diclofenac sodium (DS) is an important non-steroidal anti-inflammatory drug. It is widely used to reduce inflammation and as an analgesic in conditions such as in arthritis or acute injuries. Due to its wide use, it is one of the pharmaceuticals most commonly found in aquatic environments.[1,2] Despite its presence in small amounts as a pharmaceutical residue in bodies of water, the potential effect on the environment should not be neglected. The complete removal of DS is impossible in conventional water treatment plants due to its high polarity and solubility in water. Thus, it is important to develop effective methods to remove DS from aquatic environments.

So far, a variety of methods such as adsorption,[3–7] biodegradation,[8] oxidation,[9] and membrane filtration[10] have been employed to remove different organic micropollutants from wastewater. Amongst these techniques, adsorption using solid adsorbents is an effective method for the removal of organic micropollutants from water.[11] One of the most commonly used adsorbents for the removal of contaminants is activated carbon (AC).[12,13] However, AC has lack of adsorption selectivity and difficulty in regeneration, which limit its applications in the removal of organic micropollutants. Additionally, ion exchange resins,[14] clay minerals,[15] and some inorganic materials with mesoporous structures, such as hexagonal mesoporous silicates have also been used to remove micropollutants.[16] The adsorption procedures for these adsorbents are however, time consuming. Therefore, the development of high performance, low cost adsorbents has attracted fair amount of interest, in the treatment of organic pharmaceuticals.

Nanoparticles are used as adsorbents because of their small particle sizes, large specific surface areas and high density of surface active sites, good hydrodynamic performances.[17,18] These nanomaterials such as Fe_3O_4 nanoparticles,[19] SiO_2-coated Fe_3O_4 nanocomposites,[20,21] and carbon nanotubes[22] have been used for the removal of organic pollutants and DS in water. However, these nanoparticles adsorbents have some shortcomings, such as high preparation cost, strict operational condition, and high energy consumption. These drawbacks restrict the application of nanoparticles adsorbents in wastewater treatment. In recent years, the polymers and polymeric nanoparticles containing various functional groups, such as carboxyl (–COOH), hydroxyl (–OH), and amino ($–NH_2$), have been used for removing various kinds of contaminations from waste water.[23–26] The imprinted microspheres and nanoparticles have been synthesized for the extraction of DS from human urine.[27] So far, the polymeric nanoparticles containing quaternary ammonium salts for removal of DS have not been reported.

In this paper, from the viewpoint that possibly existed electrostatic attraction between the adsorbents and DS, the polymeric nanoparticles containing quaternary ammonium (PNPs) were synthesized by precipitation polymerization using [2-(methacryloyloxy)-ethyl]trimethylammonium chloride and

Key Laboratory of Synthetic & Natural Functional Molecular Chemistry of the Ministry of Education, College of Chemistry & Material Science, Northwest University, No. 1 Xuefu Road, Xi'an 710127, Shanxi, China. E-mail: xiezhihai8@163.com; Fax: +86-029-81535026; Tel: +86-029-8303287

ethylene glycol dimethacrylate for adsorption of DS. The adsorption and desorption of the PNPs for DS were studied in detail. The adsorption models were simulated, so as to establish the kinetic and thermodynamic equations.

2 Experimental

2.1 Chemicals and materials

Diclofenac sodium (DS), ibuprofen, naproxen, meclomen, phenylacetic acid, [2-(methacryloyloxy)ethyl]trimethylammonium chloride (DMC), and dimethyldiallylammonium chloride (DADMAC) were purchased from Aladdin Chemical Reagent (Los Angeles, USA). Ethyleneglycol dimethacrylate (EGDMA) was supplied by Xiya Reagent (Chengdu, China). 2,2′-Azobisisobutyronitrile (AIBN) was obtained from Shanpu Chemical Industry (Shanghai, China). Hydrochloric acid, sodium hydroxide, methanol, and ammonia solution (28.0%) were provided by Kemiou Chemical Reagent (Tianjin, China). Standard stock solution of DS (1000.0 mg L^{-1}) was prepared by dissolving of 0.1000 g DS in 100.0 mL deionized water. Standard working solutions were prepared by appropriate dilutions of the stock solution. Deionized water was used for the preparation of all the solutions.

2.2 Apparatus

Absorbances were recorded on a UV-2550 spectrophotometer using a 1.0 cm quartz cell (Shimadzu, Japan). The FTIR spectra of the sample, in the form of KBr pellets, were obtained by a Tensor 27 spectrometer (Bruker, Germany). The SEM image was investigated by SU-8010 SEM (Hitachi, Japan). TEM images were obtained using a H-600 TEM (Hitachi, Japan). Zeta potential values were determined by a DB-525 Analyzer (Brookhaven, USA). Fluorescence intensities were recorded using a F-4500 fluorospectrophotometer (Hitachi, Japan). The specific surface area was determined by a TriStar II 3020 surface area analyzer (Micromeritics, America). The thermal stability was measured using a STA 449C thermogravimetric analyzer (Netzsch, Germany).

2.3 Synthesis of the polymer nanoparticles

PNPs were prepared by precipitation polymerization method. DMC and EGDMA were added to 50 mL of methanol/water solution (4 : 1, v/v), and stirred at room temperature for 30 min. This was followed by the addition of AIBN (40 mg) initiator. The polymerization was allowed to proceed under nitrogen atmosphere while stirring at 55 °C for 12 h. The product was washed with methanol and deionized water, respectively. And then the product was dried under vacuum at 80 °C.

2.4 Adsorption experiment

PNPs (30.0 mg) and DS (500.0 mg L^{-1}, 25.0 mL, pH 7) were taken in a 50 mL beaker. The mixture was stirred for 7 min at room temperature and then filtered. The concentration of DS in the filtrate was measured spectrophotometrically at 275 nm. The adsorption capacity was calculated using the following equation:

$$Q = \frac{(C_0 - C_e)}{m} V \quad (1)$$

where Q (mg g^{-1}) is the adsorption capacity of PNPs, C_0 (mg L^{-1}) and C_e (mg L^{-1}) are the initial and equilibrium concentrations of DS, respectively. V (L) is the volume of the solution and m (g) is the amount of PNPs.

3 Results and discussion

3.1 The selection of monomer

DS is organic acid and can exist in water in the forms of anions or neutral molecules at different pH values ($pK_a = 4.2$). Therefore, the cationic monomers, DMC and DADMAC were chosen to prepare two different kinds of PNPs to obtain high adsorption efficiency. A series of PNPs (PNPs/DMC or PNPs/DADMAC) were prepared using different molar ratios of DMC : EGDMA or DADMAC : EGDMA. The maximum adsorption capacity of PNPs/DMC was 334.2 mg g^{-1} with 4 : 5 molar ratio of DMC and EGDMA, and the PNPs/DADMAC was only 19.87 mg g^{-1}. Therefore, DMC was chosen as cationic monomer, and the PNPs (PNPs/DMC) were prepared with a 4 : 5 (DMC : EGDMA) molar ratio in further experiments. The schematic representation of synthesis of the PNPs was illustrated in Fig. 1.

3.2 Characterization of PNPs

The FTIR spectrum of PNPs was shown in Fig. 2. The peaks at 2960 cm^{-1} and 2990 cm^{-1} could be assigned to the symmetric and asymmetric stretching vibrations of C–H of the methylene

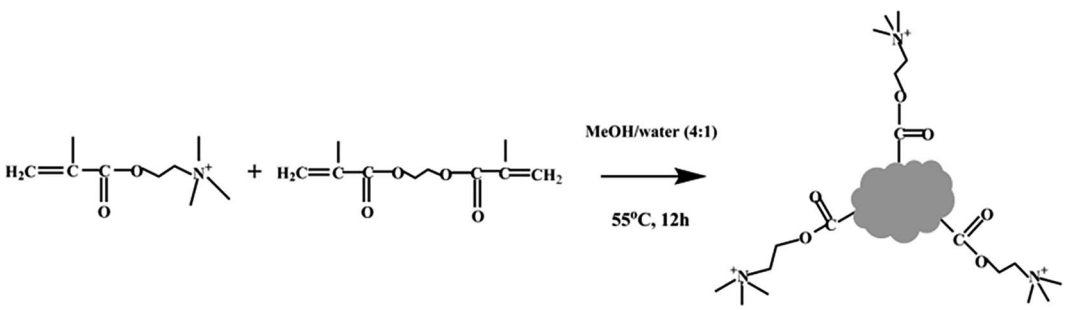

Fig. 1 Schematic representation of the synthesis of PNPs.

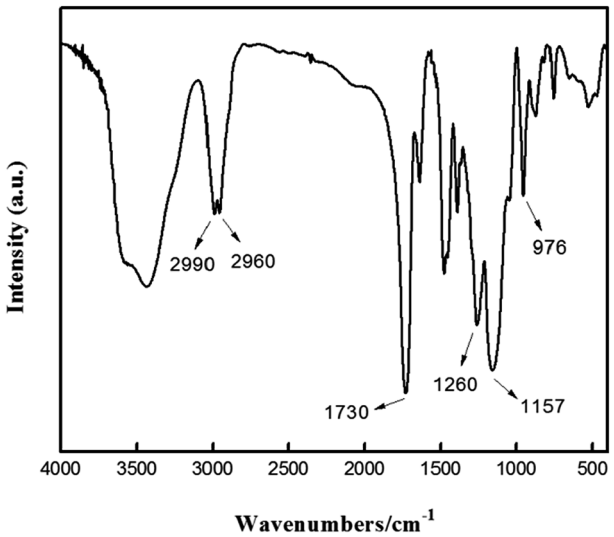

Fig. 2 FT-IR spectrum of PNPs.

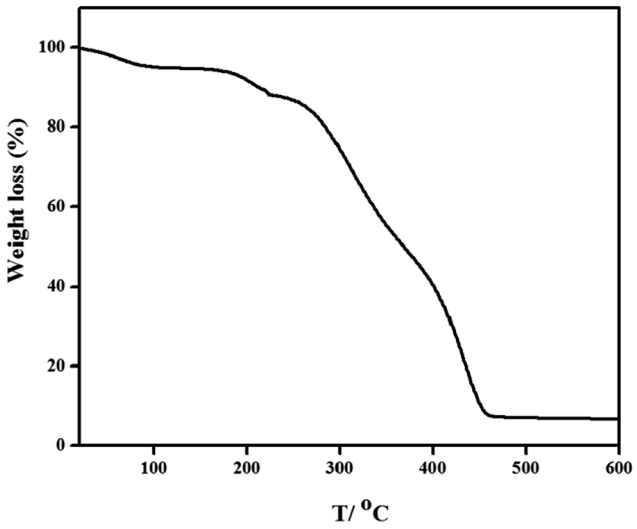

Fig. 4 The thermogravimetric analysis curves of PNPs.

groups, and the strong stretching vibration peak at 1730 cm^{-1} was due to C=O of the ester group.[28] The peaks due to the symmetric and asymmetric stretching vibrations of C–O appeared at 1260 cm^{-1} and 1157 cm^{-1}, respectively. The peak at 976 cm^{-1} was the stretching vibration of C–N in DMC.[29] These results indicated that PNPs were formed due to the co-polymerization of DMC and EGDMA.

The SEM and TEM images of PNPs were shown in Fig. 3. The diameters of the polymeric particles were in the range of 30–60 nm and the shape of granules was irregularly spherical. The PNPs were agglomerate with each other.

The specific surface area of the PNPs was determined by N_2 adsorption–desorption measurement. The specific surface area for the PNPs was 192.5 $m^2\ g^{-1}$.

The thermogravimetric analysis (TGA) curve was shown in Fig. 4. The TGA curve of the PNPs showed two weight loss stages from 20 °C to 600 °C. The first weight loss stage in the temperature range of 20–220 °C was due to the dehydration of the water residues in the PNPs. The high weight decrease in the second stage from 220 to 600 °C was assigned to the loss of the PNPs.

3.3 Adsorption properties

3.3.1 Effect of pH. Solution pH is an important factor in the adsorption process. For this, DS solutions (500.0 mg L^{-1}, 25.0 mL) with different pH values (pH 2.0 to 12.0) were prepared to investigate the effect of pH on the adsorption characteristics of PNPs. The results were shown in Fig. 5. The adsorption capacities of DS on PNPs increased with the increasing pH. When the pH was between 5.0 and 8.0, the adsorption capacity reached its

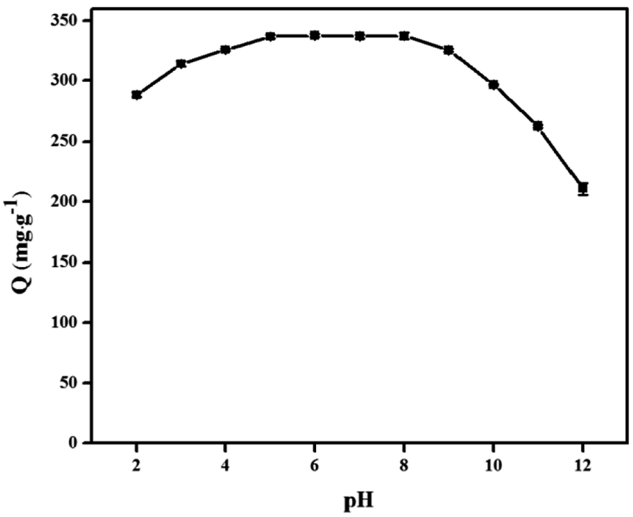

Fig. 5 Effect of pH on the adsorption capacity. Conditions: PNPs, 30.0 mg; DS, 500.0 mg L^{-1}; stirring time, 7 min.

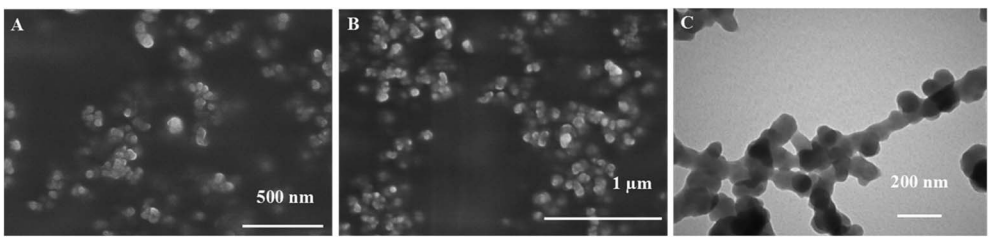

Fig. 3 SEM images (A and B) and TEM image of PNPs (C).

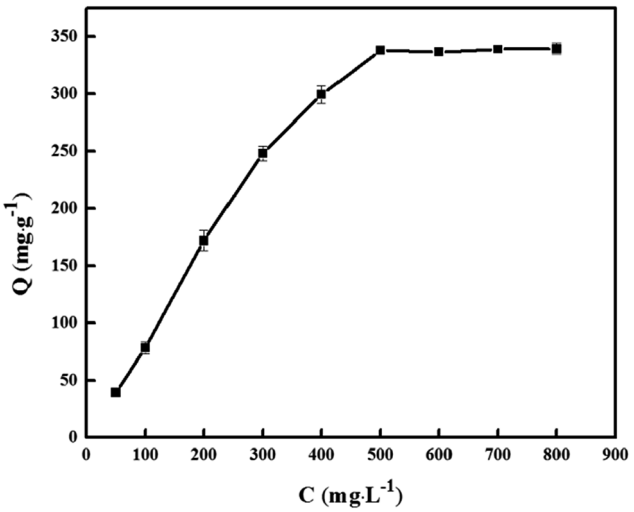

Fig. 6 Isothermal adsorption curve of PNPs. Conditions: PNPs, 30.0 mg; pH 7.0; stirring time, 7 min.

maximum value and remained constant. At pH > 8.0, the adsorption capacities decreased gradually with the increase pH. The further adsorption experiments were carried out at pH 7.

3.3.2 Adsorption isotherms. The isothermal adsorption experiments were carried out by varying the initial concentrations of DS from 50.0 to 800.0 mg L^{-1} (pH 7.0) at room temperature. The results were presented in Fig. 6. The adsorption capacity of DS on PNPs increased with the increase of DS initial concentration. When the concentration of added DS increased to 500.0 mg L^{-1}, the adsorption capacity remained constant, indicating that the active sites on the PNPs were saturated.[30] The saturated adsorption capacity of DS on PNPs was 334.2 mg g^{-1}.

Table 1 Langmuir and Freundlich constants for the adsorption of PNPs

	Langmuir			Freundlich		
T/K	K_L (L mg^{-1})	Q_{max} (mg g^{-1})	R^2	K_F (mg g^{-1})	n	R^2
283	0.1578	343.1	0.9932	72.21	3.126	0.7345
293	0.1663	344.8	0.9996	73.11	3.323	0.7253
303	0.1723	345.2	0.9821	74.45	3.561	0.7521
313	0.1803	345.6	0.9978	75.56	3.589	0.7657

In addition, the adsorption capacities of PNPs for the structural analogues of DS, such as ibuprofen, naproxen, meclomen and phenylacetic acid (Fig. 7) were also determined under non-competitive conditions at room temperature (pH 7). The saturated adsorption capacity were 117.5 mg g^{-1}, 200.3 mg g^{-1}, 184.3 mg g^{-1} and 105.3 mg g^{-1}, respectively. The PNPs have good adsorption capacities to the analogues, but the tendency of PNPs to bind DS is greater than the other examined in this study under the same conditions.

The Langmuir and Freundlich adsorption isotherm models were used to analyze the adsorption behaviors of DS on PNPs. The thermodynamic data at different temperatures were listed in Table 1. The Langmuir model was better fitted to the

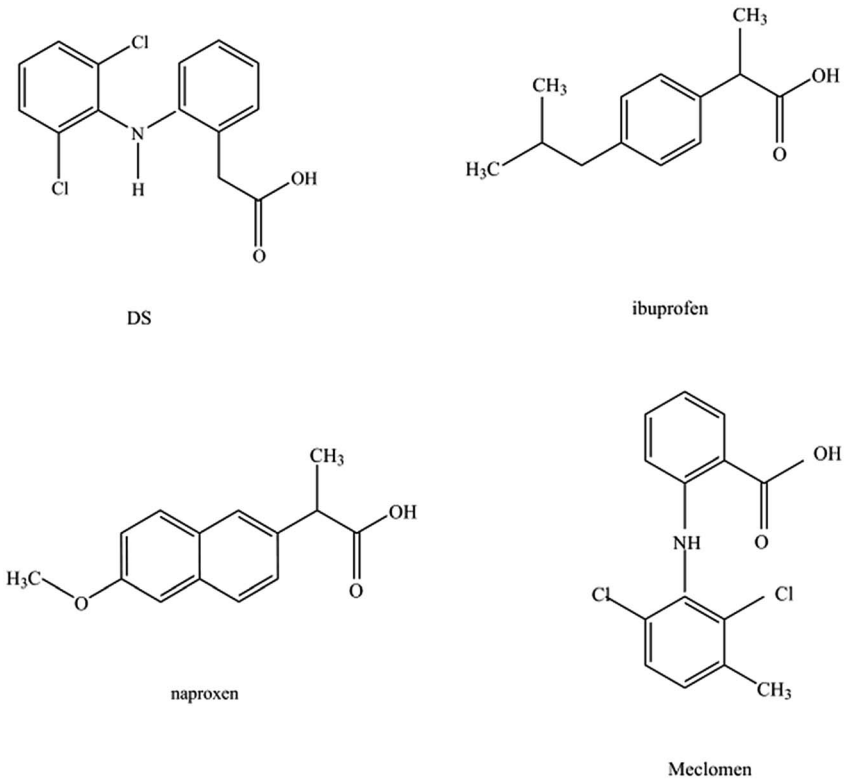

Fig. 7 Molecular structures of DS, ibuprofen, naproxen and meclomen.

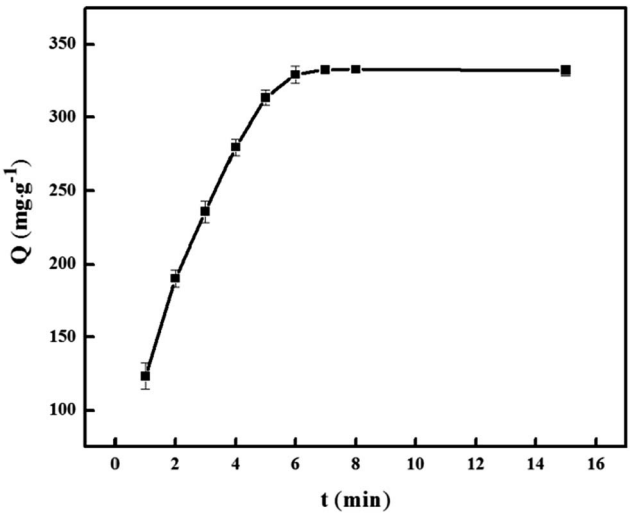

Fig. 8 Kinetics of adsorption of PNPs. Condition: PNPs, 30.0 mg; DS, 500.0 mg L^{-1}; pH 7.0.

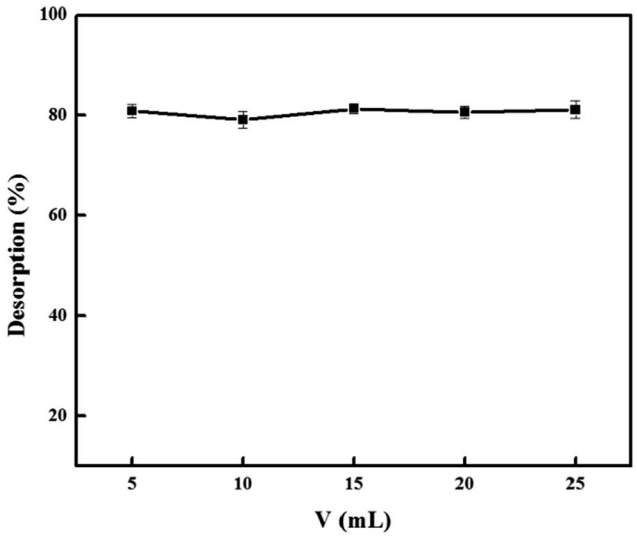

Fig. 9 Effect of elution volume on desorption efficiency. Condition: PNPs, 30.0 mg; DS, 500.0 mg L^{-1}; volume, 25.0 mL; pH 7.0; stirring time, 7 min; desorption time, 3 min.

adsorption isotherms of DS than the Freundlich model at the investigated temperatures, since the R^2 values of the Langmuir isotherm model were greater than those of the Freundlich isotherm model. The calculated value of 344.8 mg g^{-1} ($Q_{e,cal}$), estimated from the Langmuir adsorption isotherm model, was close to the experimental value of 334.2 mg g^{-1} ($Q_{e,exp}$). The results illustrated that monolayer adsorption was the main mechanism of adsorption of DS on the PNPs.[31]

3.3.3 Adsorption kinetics. The effect of the adsorption time on the adsorption capacity of the PNPs was investigated by varying the stirring time (1–15 min). Fig. 8 showed that the rate of adsorption was fast and reached about 90% of the equilibrium adsorption capacity within five minutes, due to large numbers of adsorption sites on the PNPs. Afterwards, the adsorption rate decreased and approached equilibrium after 6 min. Therefore, a time period of 7 min was chosen as the adsorption time in the following experiments.

To further study the adsorption kinetics of the PNPs for DS (whether the adsorption is dominated by a physical or chemical mechanism), the pseudo-first-order and pseudo-second-order equation were used to fit the experimental data.

The experimental data were fitted to the kinetics models mentioned above, and the obtained parameters were listed in Table 2. The value of R^2 in the pseudo-second-order model was closer to 1 than that of pseudo-first-order model. The results indicated that the applicability of the pseudo-second-order kinetic model was feasible for describing the adsorption process of DS on PNPs, which suggested that the adsorption rate was controlled by chemical adsorption.[32]

Table 2 Kinetics parameters

Kinetic models	Kinetic equation	Q_e (mg g^{-1})	k	R^2
Pseudo-first-order	$\ln(Q_e - Q) = -0.3672t + 5.0049$	148.9	0.3672/ (min^{-1})	0.6038
Pseudo-second-order	$t/Q = 0.002632t + 0.0040124$	380.2	0.001725/ (mg g^{-1} min^{-1})	0.9844

3.4 Desorption properties

3.4.1 Choice of the eluent. In the desorption experiment, the choice of eluent is important for rapid desorption. PNPs (30.0 mg) were added to DS solution (500.0 mg L^{-1}, 25.0 mL), the mixture was stirred for 7 min. Then PNPs were separated from the mixture, and added to 10.0 mL of eluent and stirred for 3 min. After separation, the concentration of DS in the eluent was determined and the elution efficiency was calculated.[33]

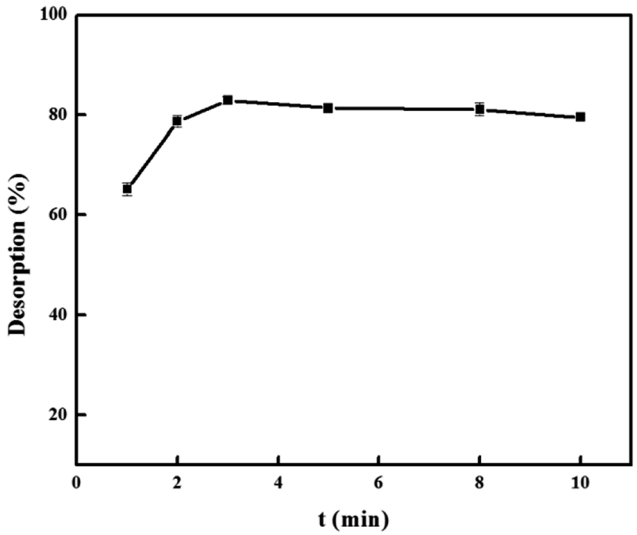

Fig. 10 Effect of desorption time on the desorption efficiency. Condition: PNPs, 30.0 mg; DS, 500.0 mg L^{-1}; volume, 25.0 mL; pH 7.0; stirring time, 7 min; eluent volume, 5.0 mL.

Table 3 Effect of reused times on the adsorption capacity

Times	1	2	3	4	5	6
Q (mg g^{-1})	334.2	331.7	329.5	326.4	323.1	322.5

Using methanol/0.3 mol L^{-1} HCl (1 : 1, v/v) as the eluent, the maximum elution efficiency of 40.21% was achieved. Methanol/0.1 mol L^{-1} ammonia (1 : 1, v/v) as the eluent, the elution efficiency was 62.97%. The solutions containing methanol/NaOH solutions (1 : 1, v/v) with different concentrations of NaOH (0.01 to 0.5 mol L^{-1}) were selected as the eluents. The elution efficiency reached 81.58% when NaOH solution was 0.1 mol L^{-1}. Thus, the solution containing equal volumes of methanol and 0.1 mol L^{-1} NaOH was chosen as the eluent in the later experiments.

3.4.2 Volume of eluent and elution time. The volume of eluent is also an important factor that affects the efficiency of the elution. In order to study this factor, the different volumes of methanol/0.1 mol L^{-1} NaOH (1 : 1, v/v) in the range of 5.0, 10.0, 15.0, 20.0, and 25.0 mL were tested and the results were shown in Fig. 9. It was found that 5.0 mL was sufficient for complete desorption of DS. To ensure that desorption of DS from the PNPs was complete, the elution time was investigated in the 1–10 min. As shown in Fig. 10, it was observed that the complete elution was achieved after 3 min.

3.5 Regeneration of PNPs

The reusability of adsorbent is an important parameter for commercial applications, especially for cost-effectiveness. To determine the reusability of PNPs, adsorption and desorption experiments were carried out for 6 cycles. From Table 3, the adsorption capacity decreased to only 3.5% in sixth cycle, as compared to the first cycle. The results indicated that the PNPs had excellent stability and practical application.

3.6 Maximum sample volume and enrichment factor

In order to obtain a higher enhancement factor, the possibility of adsorption for DS from the large sample volume was examined. For this purpose, different volumes (200–1000 mL) of sample containing 0.05000 mg DS were subjected to the adsorption procedure while the volume of eluent was kept constant at 5.0 mL. It was found that up to 1000.0 mL of aqueous sample the recovery was quantitative (>90%). Thus, the

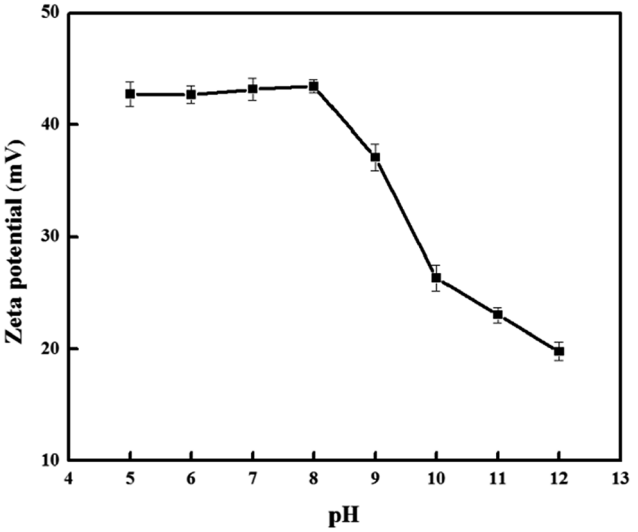

Fig. 11 Zeta potential of PNPs. Conditions: PNPs, 30.0 mg; volume, 25.0 mL.

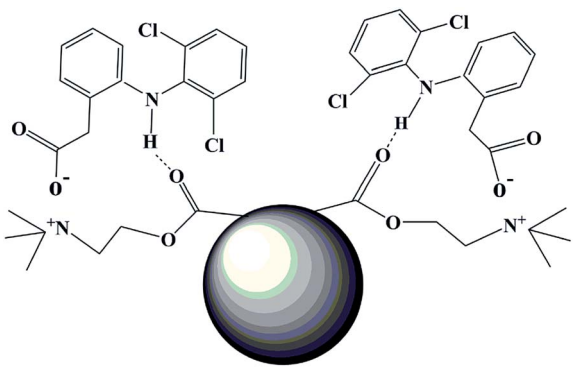

Fig. 12 Plausible mechanism for adsorption of DS on PNPs.

Table 4 Effect of coexisting substances ([DS] = 50.0 mg L^{-1})

Interfering substances	Concentration (mg L^{-1})	Relative error (%)	Interfering substances	Concentration (mg L^{-1})	Relative error (%)
Na^+	2000	1.6	Cl^-	2000	3.4
K^+	2000	3.2	SO_4^{2-}	500	4.1
Ca^{2+}	1000	1.1	NO_3^-	1000	3.1
Mg^{2+}	1000	2.6	CO_3^{2-}	1000	2.2
Al^{3+}	200	1.8	Glucose	300	−1.9
Fe^{2+}	100	−2.7	Saccharose	250	−4.7
Cu^{2+}	100	−2.2	Starch	250	−2.9
Mn^{2+}	100	−1.7	Uric acid	50	−4.2
Zn^{2+}	100	−2.8	Urea	150	−2.8
SDBS[a]	450	−1.2	OP-10	400	−3.2

[a] Sodium dodecyl benzene sulfonate.

Table 5 Comparison with other sorbents

Sorbents	Q_{max} (mg g^{-1})	Adsorption time (min)	Desorption time (min)	Enrichment factor	Ref.
Activated carbon	8.799	30	—	—	12
Carbon nanotube	24.01	60	—	—	22
Bentonite hybrid material	18.99	15	—	—	16
Carbon xerogel	80.0	2880	—	—	9
Ion exchange resins	3.18	1440	—	—	14
Nanoparticles polymer	150.4	40	—	4	27
Magnetic polymer	116.0	6	7	100	20
2-Vinylpyridine polymer	324.8	120	—	500	2
1-Vinylimidazo polymer	10.32	60	10	10	23
Methacrylic acid polymer	—	30	8	100	24
Clay mineral	15.9	1440	—	—	15
PNPs	334.2	7	3	200	This work

sample volume of 1000 mL could be subjected to the adsorption procedure and the enrichment factor for DS was 200 by this method.

3.7 Effect of coexisting substances

Under the optimal conditions, various coexisting substances were examined for effect on the adsorption capacity of PNPs for DS. The permitted relative deviation from adsorption capacity was ±5%. The experimental results were summarized in Table 4. The results show that the coexisting substances normally present in water do not interfere.

3.8 Adsorption mechanism

Understanding the adsorption mechanism is important, not only to understand the basics of adsorption but commercial applications of adsorption technologies. From Fig. 5, the adsorption capacity at pH values lower than the pK_a of DS was smaller than that at pH of 5.0, because DS was in the form of neutral molecules (–COOH). On increasing the pH from 5.0 to 8.0, the adsorption capacity reached maximum and kept constant due to DS in the form of anions ($–COO^-$) at pH > pK_a, finally decreased at pH > 8.0. The zeta potential of the PNPs (shown in Fig. 11) indicated that there was a positive surface charge on PNPs over a wide pH range, but surface positive charge decreased at pH > 8.0. It was also consistent with the result that the adsorption capacities decreased gradually with the increase of pH due to the decrease of surface positive charge of PNPs from 9.0 to 12.0. The results suggested that the electrostatic interactions between anionic DS and cationic PNPs could be the main driving forces for adsorption. In addition, the hydrogen of secondary amine in DS molecule combined with the oxygen atom in the carbonyl group of PNPs by hydrogen bonds.[34] Therefore, plausible adsorption mechanism is shown in Fig. 12.

3.9 Comparison with other sorbents

The prepared PNPs sorbent was also compared with other sorbents reported in literature. The comparison of adsorption capacities, adsorption times, desorption times and enrichment factors of different kinds of sorbents, were presented in Table 5. It was clear that the adsorption capacity of the PNPs, prepared in this study, was much higher. Additionally, adsorption time and desorption time were also very fast, because of the nature of nanoparticles.

4 Conclusions

In this paper, PNPs were synthesized using DMC and EGDMA, by precipitation polymerization method. The prepared PNPs were utilized to adsorb DS. The most significant characteristics of PNPs were high adsorption capacity, fast adsorption and desorption of DS, probably due to the nature of its nanoparticles. It was speculated that PNPs could be utilized as a potential sorbent for separation and enrichment DS from aquatic environments.

Conflict of interest

The authors declare no competing financial interest.

References

1 L. Figueiredo, G. L. Erny, L. Santos and A. Alves, *Talanta*, 2016, **146**, 754–765.
2 C. M. Dai, X. F. Zhou, Y. L. Zhang, S. G. Liu and J. Zhang, *J. Hazard. Mater.*, 2011, **198**, 175–181.
3 B. C. Pires, F. V. A. Dutra, T. A. Nascimento and K. B. Borges, *React. Funct. Polym.*, 2017, **113**, 40–49.
4 M. J. Ahmed, *J. Environ. Manage.*, 2017, **190**, 274–282.
5 A. Khan, J. Wang, J. Li, X. Wang, Z. Chen, A. Alsaedi and X. Wang, *Environ. Sci. Pollut. Res.*, 2017, **24**, 1–21.
6 M. Zhou, Q. Li, S. Zhong, J. Chen, H. Lin and X. L. Wu, *Mater. Chem. Phys.*, 2017, **198**, 186–192.
7 X. L. Wu, P. Xiao, S. Zhong, K. Fang, H. Lin and J. Chen, *RSC Adv.*, 2017, **7**, 28145–28151.
8 S. T. Lee, B. Yang, J. Y. Kim, J. H. Park and M. H. Moon, *J. Chromatogr. A*, 2015, **1409**, 218–225.
9 S. Álvarez, R. S. Ribeiro, H. T. Gomes, J. L. Sotelo and J. García, *Chem. Eng. Res. Des.*, 2015, **95**, 229–238.

10 N. Suriyanon, P. Punyapalakul and C. Ngamcharussrivichai, *Chem. Eng. J.*, 2013, **214**, 208–218.
11 S. W. Nam, C. Jung, H. Li, M. Yu, J. R. Flora, L. K. Boateng and Y. Yoon, *Chemosphere*, 2015, **136**, 20–26.
12 S. Larous and A. H. Meniai, *Int. J. Hydrogen Energy*, 2016, **41**, 10380–10390.
13 J. L. Sotelo, G. Ovejero, A. Rodríguez, S. Álvarez, J. Galán and J. García, *Chem. Eng. J.*, 2014, **240**, 443–453.
14 K. A. Landry, P. Sun, C. H. Huang and T. H. Boyer, *Water Res.*, 2015, **68**, 510–521.
15 K. Sun, Y. Shi, H. Chen, X. Wang and Z. Li, *J. Hazard. Mater.*, 2017, **323**, 567–574.
16 D. Tiwari, *Chem. Eng. J.*, 2015, **263**, 364–373.
17 X. L. Wu, P. Xiao, S. Zhong, K. Fang, H. Lin and J. Chen, *RSC Adv.*, 2017, **7**, 28145–28151.
18 L. Ma, Y. Peng, B. Wu, D. Lei and H. Xu, *Chem. Eng. J.*, 2013, **225**, 59–67.
19 S. Ansari and M. Karimi, *Talanta*, 2017, **167**, 470–485.
20 A. A. Pebdani, A. M. H. Shabani and S. Dadfarnia, *J. Iran. Chem. Soc.*, 2016, **13**, 155–164.
21 X. L. Wu, Y. Shi, S. Zhong, H. Lin and J. R. Chen, *Appl. Surf. Sci.*, 2016, **378**, 80–86.
22 X. Hu and Z. Cheng, *Chin. J. Chem. Eng.*, 2015, **23**, 1551–1556.
23 V. Manzo, K. Ulisse, I. Rodríguez, E. Pereira and P. Richter, *Anal. Chim. Acta*, 2015, **889**, 130–137.
24 A. A. Pebdani, A. M. H. Shabani, S. Dadfarnia and S. Khodadoust, *Spectrochim. Acta, Part A*, 2015, **147**, 26–30.
25 Y. He, T. Xu, J. Hu, C. J. Peng, Q. Yang, H. L. Wang and H. L. Liu, *RSC Adv.*, 2017, **7**, 30500–30505.
26 X. Song, L. Li, Z. Geng, L. Zhou and L. Ji, *J. Environ. Chem. Eng.*, 2017, **5**, 16–25.
27 S. Noee, N. Salimraftar, M. Abdouss and G. Riazi, *Polym. Int.*, 2013, **62**, 1711–1716.
28 S. Sadeghi and M. Jahani, *Food Chem.*, 2013, **141**, 1242–1251.
29 M. M. Gou, L. Shen and Y. J. Xing, *Dyeing Finish.*, 2012, **38**, 6–9.
30 C. M. Dai, S. U. Geissen, Y. L. Zhang, Y. J. Zhang and X. F. Zhou, *Environ. Pollut.*, 2011, **159**, 1660–1666.
31 F. Hayeeye, M. Sattar, W. Chinpa and O. Sirichote, *Colloids Surf., A*, 2017, **513**, 259–266.
32 J. Fu, Z. Chen, M. Wang, S. Liu, J. Zhang, J. Zhang, R. P. Han and Q. Xu, *Chem. Eng. J.*, 2015, **259**, 53–61.
33 Y. Zhang, Z. H. Xie, X. X. Teng and J. Fan, *J. Sep. Sci.*, 2016, **39**, 1559–1566.
34 Z. H. Xiong, L. Wang, J. G. Zhou and J. M. Liu, *Acta Phys.-Chim. Sin.*, 2010, **26**, 2890–2898.